SOME CONSIDERATIONS ON THE INTEGRATION OF ENGINE NACELLES INTO LOW-BOOM AIRCRAFT CONCEPTS

Robert J. Mack
NASA Langley Research Center
Hampton, VA

SUMMARY

A study of wind-tunnel data has shown why unexpected strong shock waves appeared in the wind tunnel pressure signatures of two low-boom models, and has indicated that changes to the current methods for analyzing and designing low-boom aircraft are needed. The discussion provided corrections for the interference lift code, and suggested methods of treatment for the equivalent areas of the aircraft, especially the nacelles and the interference lift, which were to be used in the aircraft design and the sonic boom analysis.

INTRODUCTION

The first low-boom theory validation bodies that departed from the body-of-revolution format by including lift effects were simple wing-fuselage models[1]. They were built to test the minimum sonic boom theory of Seebass and George[2], and the variable nose blunting modification of Darden[3]. Results from the wind tunnel tests of these models showed that, at a Mach number of 1.50, there was reasonably good agreement between theory and experiment. However, at a Mach number of 2.70, good agreement was found only in the forward half of the signatures. These less satisfactory results were attributed to the linear theory used to obtain the lift distribution. With the introduction of the modified linear theory wing analysis code, limitations associated with linearized theory were corrected and satisfactory predictions of area-ruled lift distributions were obtained[4].

As a follow-on to the low-boom validation study in reference 1, additional sophistication and complexity was employed in two low-boom models by including wing camber and twist, engine nacelles, fuselage camber, and a vertical tail in the design. Wind tunnel tests of these second-generation low-boom validation models (samples given in Appendix A) revealed unforeseen problems. The pressure signatures from these models showed unexpected strong shock waves originating from the nacelles. An initial analysis of these data suggested that a strong shock, caused by choked flow, stood in front of each nacelle inlet. However, further analysis of the low-boom model wind-tunnel data along with some supplemental isolated-nacelle wind tunnel model data indicated that this simple explanation was not the total answer. Moreover, the analysis suggested that some changes to the usual method of treating nacelle flow-field effects and nacelle-

interference lift effects in the design and analysis of supersonic-cruise aircraft[5] would be necessary.

The main purpose of this paper is to analyze these unexpected strong shock waves that have been traced to the under-the-wing nacelles. Once the reasons for the appearance of these stronger-than-expected disturbances have been identified, practical methods will be then be suggested for integrating nacelles with the wing-fuselage to keep the aircraft flow field free of finite-size shock waves except for the controlled-strength shock waves from the nose and the tail.

SYMBOLS

A_e equivalent areas, ft^2

CFD   Computer Fluid Dynamics

$F(y)$ Whitham F-function

h   distance between the model and the probe, in

M   Mach number

p   free stream pressure, psf

Δp incremental overpressure, psf

Δx distance along pressure signature, in

x_e effective distance along the longitudinal axis, ft

y   effective distance parameter in the Whitham F-function, ft

β $\sqrt{M^2 - 1}$

γ ratio of specific heats, for air, $\gamma = 1.40$

δ tangent of the flow deflection angle, see equations (1) and (3)

κ correction factor defined in equation (4b)

ξ $\Delta p / p$, see equation (2)

ξ_0 first order Whitham theory estimate of ξ , see equation (3)

DISCUSSION

The measured pressure signatures generated by the second-generation sonic boom validation models (samples in *APPENDIX A*) showed unexpected and unpredicted strong shock waves. Preliminary analysis of the data suggested that, because of their small size, the cylindrical duct within the nacelle had suffered choked flow so that a strong, detached shock stood at each nacelle inlet. Analysis of data from supplemental wind tunnel model tests with nacelles of varying sizes surfaced another possible cause of the shocks, one which would introduce extra shocks whether the flow in the nacelle constant-area duct was or was not choked.

Engine nacelles, on the wind tunnel low-boom models tested, were moderately-slender, symmetrical bodies of revolution mounted in pairs under the wing lower surface. In this near-field position, inlet lip shock waves striking the wing surface were considerably stronger than those predicted by the Whitham theory in the interference lift computer code. These direct flow field effects were complicated by the nacelle shock waves which were reflected from the wing lower surface. In designing these models, the strength of the direct and reflected nacelle-induced shock waves and the attendant flow field pressures were underestimated. So the underestimation of the reflected shock wave strengths lead to underestimated nacelle-wing interference forces. Because the sonic boom prediction code in reference 6 is based on the assumption of small-disturbance propagation, the weaker predicted strengths of the nacelle-lip shock waves were extrapolated as weak-disturbance pressure signatures from the low-boom aircraft which propagated to the ground.

The presence of strong shocks also presented a need for improved integration methods. Careful wing-fuselage blending permitted a slow steady initial growth in volume and lift equivalent area. Near the trailing edge of the lower wing surface, the nacelles initiated a pattern of abrupt, strong shocks rather than a pattern of weak, distributed-pressure disturbances. Aircraft surface realignment which would accommodate, compensate, and neutralize these shocks and their reflections would also need to be finite and rapid (rather than small and gradual), initiated well ahead of the nacelle inlet location. Any "smearing" or averaging of pressure gradients in the analysis codes would "soften" and smooth the abrupt start of the nacelle-wing interference-lift effects. Thus, the prediction codes that underestimated the shock strengths also under-prescribed the accommodation and added to the problem.

Aircraft models of sufficient size could have nacelles large enough to establish and maintain one hundred percent flow through the constant area duct. This would dispose of any problems caused by choked-inlet-flow, i.e. detached shocks, but it would still leave the problem of predicting the extreme-near-field shock strengths, from direct and reflected shock waves, to be addressed. In the following section, each of these points will be analyzed and corrections to existing methods will be suggested.

The method for determining the flow field disturbances effects of the engine nacelles on the aircraft and on the surrounding flow field required two corrections. First, the strengths of the shock waves and the pressure field in the extreme near field need to be corrected. Second, the incremental F-functions from the nacelle geometry and the interference lift must be integrated into the total aircraft volume and lift F-function.

Shock Strength Correction. The interference lift induced by the nacelles flow field on the wing lower surface is estimated by a computer code based on Whitham theory[7]. This theory has been experimentally tested and verified at distances as close as one nacelle length. However, for a nacelle whose length is six to nine mean diameters, a considerable part of the interference zone is within a radial distance of one to five nacelle diameters. The shock wave strengths and flow-field pressures predicted by the Whitham theory code at these extreme near-field distances would definitely be less than found in the real flow.

One correction, found in reference 8 from equations (151) and (174), estimates the flow-field pressure changes from weak shock and expansion theory. The first two terms in these equations are the same, and have the form

$$\frac{\Delta p}{p} = \gamma \frac{M^2 \delta}{\beta} + \gamma M^2 \frac{(\gamma + 1.0) M^4 - 4.0 \beta^2}{4.0 \beta^4} \delta^2 \tag{1}$$

Writing

$$\xi = \frac{\Delta p}{p}, \tag{2}$$

and using

$$\xi_0 = \frac{\gamma M^2 \delta}{\beta} \tag{3}$$

as the estimated magnitude of $\Delta p/p$ obtained from Whitham theory, equation (1) can be written in ratio form as,

$$\frac{\xi}{\xi_0} = 1.0 + \frac{(\gamma + 1.0) M^4 - 4.0 \beta^2}{4.0 \gamma M^2 \beta^2} \xi_0 \tag{4}$$

or more conveniently as

$$\xi = \xi_0 + \kappa \xi_0^2 \qquad (4a)$$

where

$$\kappa = \frac{(\gamma + 1.0) M^4 - 4.0\beta^2}{4.0\gamma M^2 \beta^2} \qquad (4b)$$

At best, this is an empirical nonlinear correction, but it does account for some second-order overpressure and Mach number effects. In figure 1, a plot of κ versus Mach number is shown.
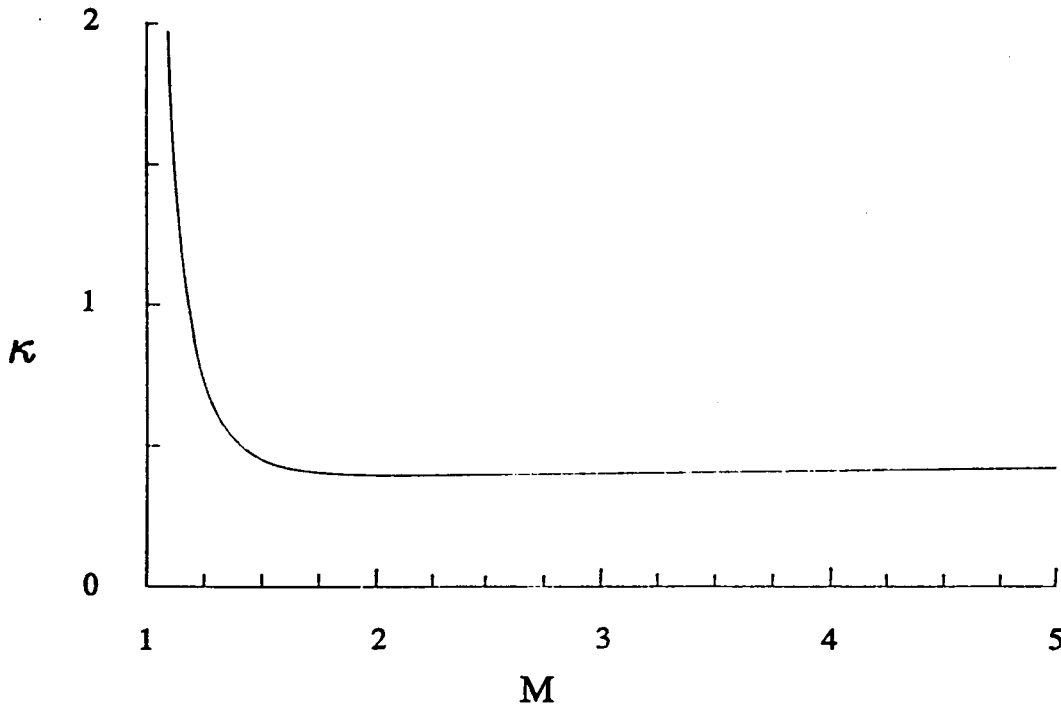

Figure 1. Mach number effects on the value of κ.

The value of κ can be significant for Mach numbers between 1.0 and 1.2, but this is where supersonic theory is not very applicable and is seldom used. Beyond a Mach number of 2.0, the value of κ is approximately 0.40 and asymptotically approaches a value of 3/7 or about 0.42857 for $\gamma = 1.40$. Note that within the usual range of Mach numbers and $\Delta p / p$ where Whitham theory is used, namely Mach numbers between 1.4 and 3.0 and $\Delta p / p = \pm 0.02$, the total correction, as found from equation (4), is approximately 1.008, very close to 1.0 as it should be for the theory to be applicable. However, in the close proximity of an engine nacelle, $\Delta p / p$ can be 0.30 and larger, in which case the correction factor is 1.12 or larger.

When the local nacelle-wing interference pressures are corrected using equation (4), a better estimate of interference lift, drag, and pitching moment is obtained. Incremental equivalent areas due to nacelle-wing interference are also more accurate. However, the problem of a rapid, local increase of equivalent area due to nacelle-wing interference still remains.

Nacelle and Nacelle-Wing Interference F-functions. The usual method for computing the F-function of the entire aircraft (and from the F-function, the pressure signature) involves adding equivalent areas from each of the components. The equivalent areas from the fuselage, wing, wing lift, and fin are added and treated as a single area distribution because they are usually blended and integrated so smoothly that they appear to the air flow as a single slender body with small perturbations along its length. Figure 2 shows Mach-sliced areas from these four components for a supersonic cruise aircraft designed to have low sonic boom ground overpressures and shock strengths.
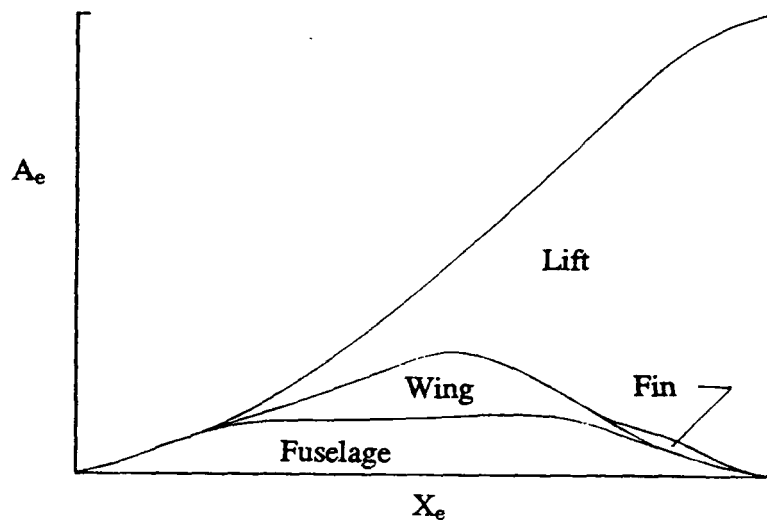

Figure 2. Equivalent areas from aircraft fuselage, wing, wing lift, and fin.

Nacelles, especially axi-symmetric ducted nacelles, are often mounted under and away from the wing or fuselage surface. The flow would "see" them as separate bodies, and therefore "see" discrete, rather than smoothly blended, disturbances.

Figure 3 is the F-function computed from the combined fuselage, the wing, the wing lift, and the fin equivalent areas shown in figure 2. The accuracy of this F-function is based on the assumption that the components have been well integrated and blended during the preliminary design procedure.

226

Figure 3. Typical F-function computed from equivalent areas in figure 2.

A three-view drawing, figure 4, shows the conceptual aircraft that is the source of the equivalent areas in figure 2 and the F-function in figure 3. On this configuration, the engine nacelles are seen in the usual under-the-wing location.
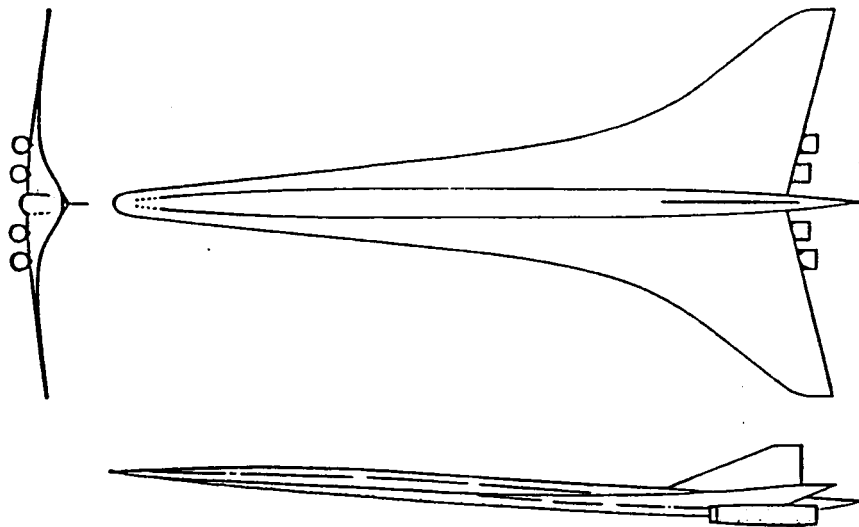

Figure 4. Three-view of a conceptual aircraft with a typical nacelle-wing arrangement.

227

Since this is a highly blended configuration, the areas and the first and the second derivatives of the fuselage, wing, wing lift, and the fin areas are usually smooth and continuous. Still, the F-function is not smooth and continuous even though there are no surface discontinuities, or "jumps" in area growth. It is due mainly to the numerical treatment of the area inputs.

Interference lift is generated in the zone bounded by the intersection of the wing lower surface and trailing edge with the nacelle inlet shock. The equivalent areas from the longitudinal nacelle-wing interference lift growth are shown in figure 5.
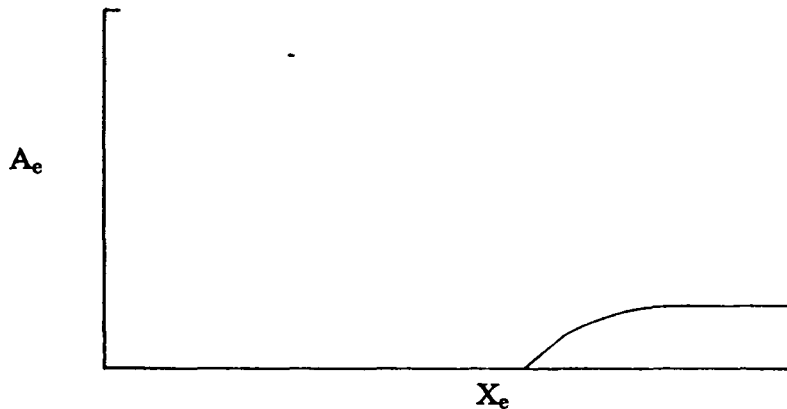
Figure 5. Equivalent areas due to nacelle-wing interference lift.

If the nacelles were slender and pointed, the initial equivalent areas would be proportional to x_e^2 and the F-function would be zero at $y = 0.0$. Since, however, the nacelles are ducted, the F-function at $y = 0.0$ is non-zero, and may be large even though the magnitude of the maximum equivalent area of the interference lift is only about $1/40^{th}$ of the wing lift for each nacelle pair. Since flow-field disturbances are determined by the weighted and integrated second derivatives of the area, the rapid growth of interference-lift equivalent area can lead to predictions of shock strengths which can rival the shock strength from the fuselage nose. The F-function computed from the nacelle-wing interference lift areas, figure 5, is shown in figure 6.
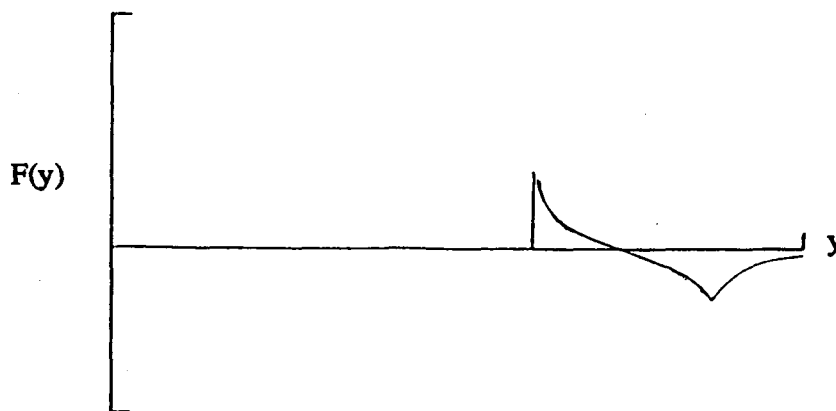

Figure 6. Computed F-function from areas specified in figure 5.

This is the F-function from just one pair of engine nacelles; there will be another F-function, similar in shape but shifted in effective length, x_e, from the other pair of nacelles on the aircraft. The flow field disturbances from the aircraft are obtained by summing the F-function components. This combined F-function is shown in figure 7.
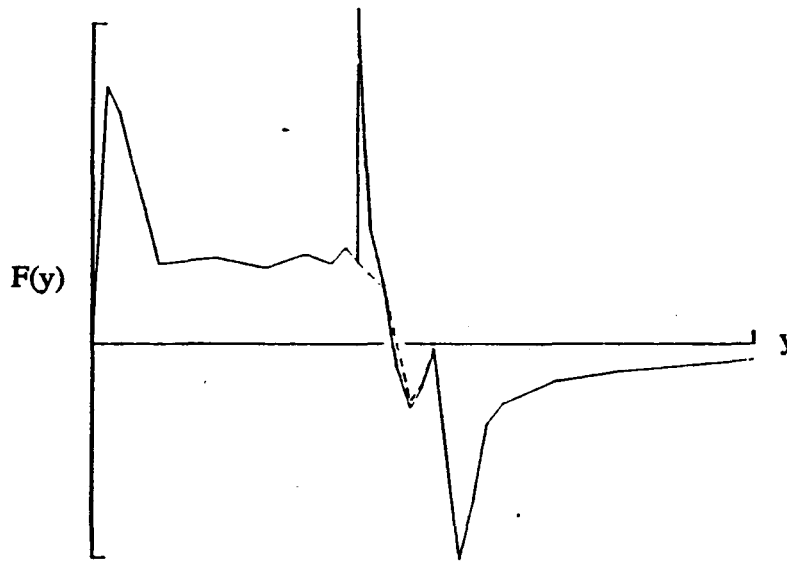

Figure 7. Combined F-function computed from fuselage, wing, wing lift, fin, and interference lift equivalent areas. (The dashed lines show the original lines in figure 6.)

If the nacelle equivalent areas were added to the fuselage, wing, wing lift, and fin equivalent areas and these total areas were used to derive an F-function, the "spikey" discontinuity would have been severely rounded and its effect on the near-field pressure predictions would have been lost.

The identification and acoustic treatment of flow field disturbance sources requires an additional step. This involves the disturbance from each nacelle as though it were an isolated body. Equivalent areas from the nacelle are shown in figure 8.
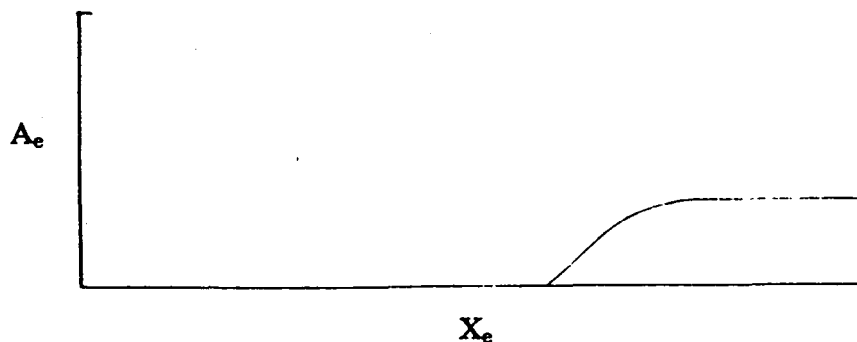

Figure 8. Isolated-nacelle equivalent areas.

229

If the engine nacelles were mounted close to the fuselage-wing surface, and integrated with careful volumetric blending to the fuselage-wing-fin airframe, their volume contribution could be computed together. In the below-the-wing position, however, lumping the nacelles with the fuselage-wing-fin results in an area distribution where the nacelle flow-field shocks and pressures are underestimated. The F-functions from the isolated nacelles are shown in figure 9.
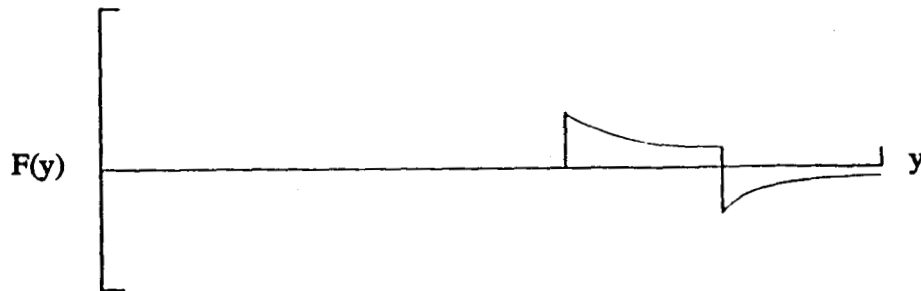

Figure 9. Isolated engine nacelle F-function computed from areas in figure 8.

When they are added to the F-function in figure 7, the total aircraft F-function shown in figure 10 is obtained.
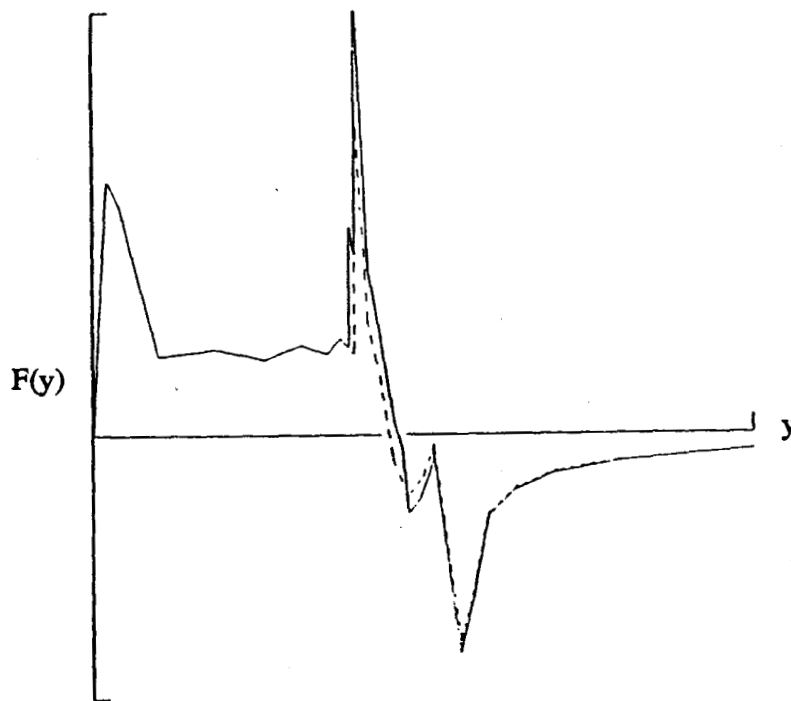

Figure 10. F-function of all aircraft components. (The dashed lines show the F-function before the increments from figure 9 were added.)

230

A typical desired F-function for a low-boom cruise aircraft is added to the F-function in figure 10 for comparison in figure 11.
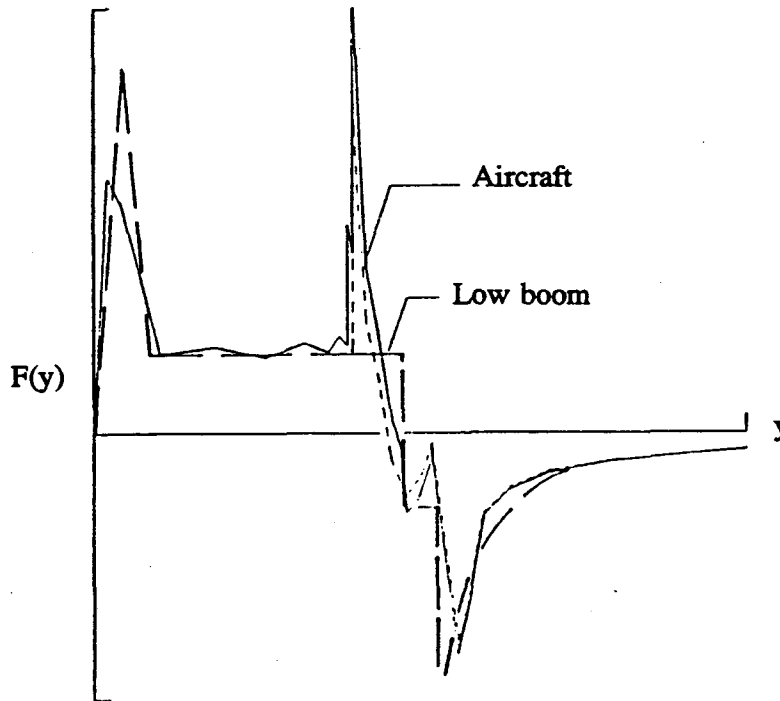

Figure 11. Comparison of aircraft and low boom F-functions. (The short dashed lines are from F-function features shown in figure 10.)

Figure 11 shows that extra shocks could have appeared in the extreme near-field measured pressure signatures even with one hundred percent flow through the nacelle ducts, and that the ideal pressure signatures would not be realized at the cruise distance with the full-scale aircraft. Engine nacelle volume and interference lift equivalent areas are a small contribution to the total equivalent areas dominated by contributions from the wing lift. Small discontinuities in area growth are almost imperceptable and can be compensated for, in most cases, by small changes in local fuselage areas. However, sizeable discontinuities in component area growth are smoothed over when all the areas are summed. Therefore, no discontinuities will appear in the F-function calculated with the summed areas even though they are required for complete accuracy.

When equivalent areas alone are considered, agreement between the aircraft's and the desired low-boom equivalent areas usually is interpreted to mean that low boom constraints have been achieved. In the larger scope of low-boom methodology, there must also be, and usually is, agreement between the aircraft's and the desired low-boom F-functions. The total aircraft equivalent areas, figure 2, were derived from the low-boom F-function with the assumption that all

components could be integrated smoothly together. Fuselage, wing, wing lift, and fin integration usually fit within the scope of these assumptions. Engine nacelles, however, do not fit these assumptions. Therefore, new techniques and/or applications of the old theory and methodology are required.

The methods used at the Langley Research Center emphasized the agreement between equivalent areas for low-boom design. This aided greatly in the integration of aircraft components to obtain a conceptual aircraft with high aerodynamic efficiency and the potential for generating low-strength ground overpressures. Methods used by others emphasized the agreement between the aircraft and the desired F-function with overall equivalent areas monitored to assure that total lift, incremental engine nacelle area differences between the exhaust and the inlet, and the fuselage wake areas were accounted for in the net flow field effect. It is now clear that a synthesis of both methods should be used to meet design objectives for obtaining practical, low-boom, conceptual aircraft configurations.

CONCLUDING REMARKS

The need for making corrections and adjustments to the methods that estimate interference lift effects has been discussed. Corrections for underestimated shock strengths and flow field pressures due to engine nacelles were derived. Additionally, the discrete-disturbance nature of the nacelle flow field was discussed and a technique for correcting the existing analysis method which predicts flow field overpressure signatures was presented. Application of both these corrections should permit more accurate predictions of ground-level sonic boom signatures and aid in the design and analysis of low-boom, supersonic cruise configurations.

Corrections to the interference lift code and revisions to the equivalent area / F-function methodology will help the problem concerning analysis procedures. The second problem, nacelle-induced shocks, will require finding nacelle shapes that produce weaker inlet lip shocks while at the same time generating practical levels of nacelle-wing interference lift whose equivalent areas "grow" initially at a more gradual rate. These two requirements may be in direct conflict but are worth investigating.

Axisymmetric and two-dimensional nacelles with under-the-wing trailing edge mounting seem to be the preferred types and location. Moving the engine nacelles from under the wing to the aft fuselage has been tried before, and now with benefits to sonic boom possible, might merit being tried again.

REFERENCES

(1) Mack, Robert J. ; and Darden, Christine M. : Wind-Tunnel Investigation of the Validity of a Sonic-Boom-Minimization Concept. NASA TP-1421, 1979.

(2) Seebass, R. ; and George, A. R. : Sonic-Boom Minimization. Journal of the Acoustic Society of America, vol. 51, no. 2, pt. 3, Feb. 1972, pp. 686-694.

(3) Darden, Christine M. : Sonic-Boom Minimization with Nose-Bluntness Relaxation. NASA TP-1348, 1979.

(4) Carlson, Harry W. ; and Mack, Robert J. : Estimation of Wing Nonlinear Aerodynamic Characteristics at Supersonic Speeds. NASA TP-1718, 1980.

(5) Mack, Robert J. ; and Needleman, Kathy E. : A Methodology for Designing Aircraft to Low Sonic Boom Constraints. NASA TM-4246, 1991.

(6) Hayes, Wallace D. ; Haefeli, Rudolph C. ; and Kulsrud, H. E. : Sonic Boom Propagation in a Stratified Atmosphere, with Computer Program. NASA CR-1299, 1969.

(7) Whitham, G. B. : The Flow Pattern of a Supersonic Projectile. Communication on Pure and Applied Mathematics, vol. V, no. 3, Aug. 1952, pp. 301-348.

(8) Ames Research Staff : Equations, Tables, and Charts for Compressible Flow. NACA Report 1135, 1953.

APPENDIX A

The following pressure signatures are samples of experimental data from two low-boom-constrained wind tunnel models. In both figures, the model is a conceptual aircraft designed to cruise at a Mach number of 2.0 at an altitude of 55,000 feet. Since this model was designed primarily to validate low-boom technology, high aerodynamic efficiency was of secondary importance.

The wind tunnel tests were conducted at conditions of a Mach number of 2.0, a total temperature of 125.0 degrees Fahrenheit, and a unit Reynolds number of 2.0 million per foot. Free-stream pressures were measured with a two-hole conical probe whose semi-vertex angle was 2.0 degrees.

In figure A-1, the model had nacelles made of a composite material. In order to maintain form and strength, the walls were thickened in an inward direction. This decreased the internal duct diameter and made the inlet lips blunter than desired. The pressure signature was measured 24.0 inches beneath the model.
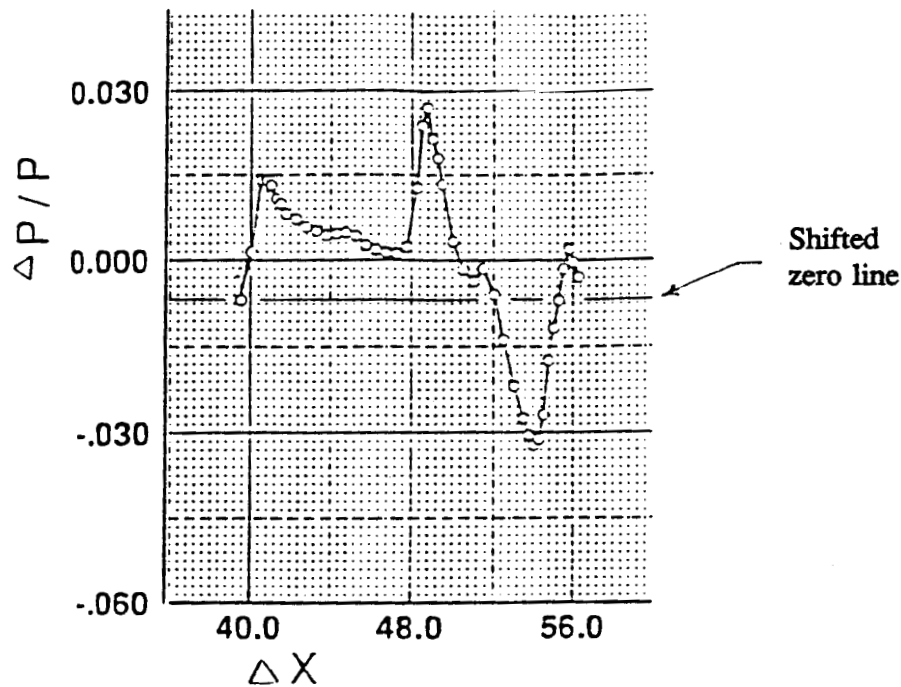
233

Figure A-1. Model with composite nacelles with h = 24.0 inches.

Note: There is a shifted-zero line on the data plot. Several reference-pressure data points were selected to be the basis for the reference axis. Some were incorrect and were removed. However, the old zero-pressure line remained in place, and was noticed after the paper was prepared.

There are several interrelated effects causing the strong shocks from the nacelles. The first is the blunt inlet lips, the second effect is possibly due to the reduced internal duct area, and a third possible effect could be due to the reduced Mach number of the flow field under the wing aggravating conditions leading to the previous effects. Two of these effects are relieved by using nacelles with adequate diameters and sharp inlet lips.

In figure A-2, the model had stainless steel nacelles with an inlet lip edge radius made to about 0.003 inch tolerances.
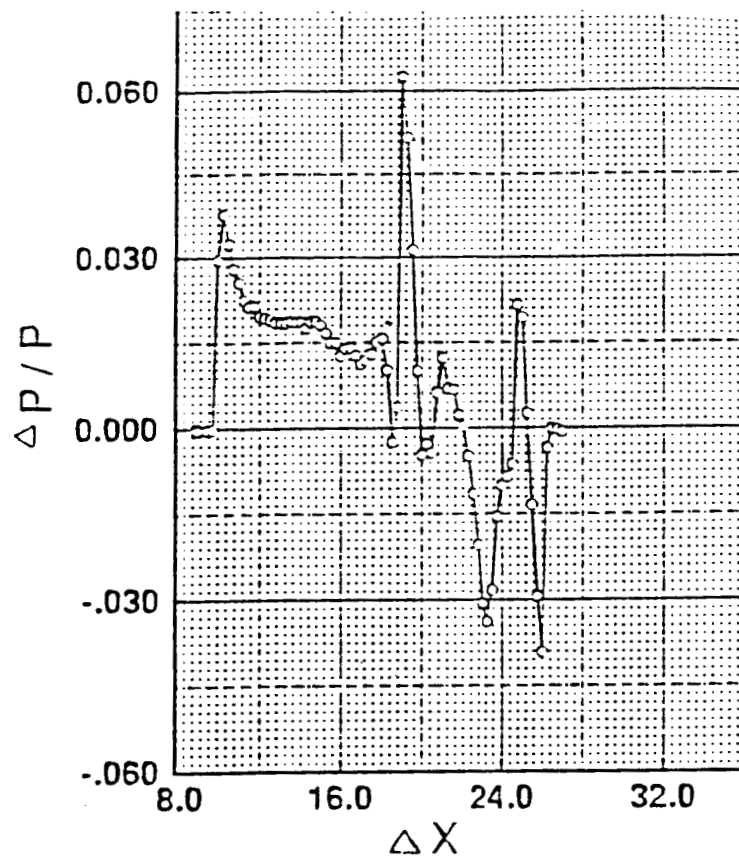
Figure A-2. Model with sharp-lip nacelles at h = 6.0 inches.

In both figures, the pointed, well-defined pressure peak after the nose shock defines the disturbances caused by the nacelles.